

Inhibited Under-Deposit CO₂ Corrosion: Small Particle Silica Sand and Eicosane Paraffin Deposits

Shokrollah Hassani, Jin Huang, Ana Camila Victor, Bruce Brown, and Marc Singer
Institute for Corrosion and Multiphase Technology, Ohio University
342 W. State Street
Athens, OH 45701
USA

ABSTRACT

Chemical inhibition in the presence of silica sand deposit has been reported as a cause of severe localized corrosion attack in CO₂-saturated brine environments. This paper suggests a new mechanism for explaining physics behind the localized corrosion attack based on experimental evidences. The effect of sand size and deposit type on localized corrosion attack in the presence of imidazoline type inhibitor is also experimentally investigated in CO₂-saturated brine solution. Smaller silica sand particles (diameter less than 44 micron) are found to cause less localized corrosion attack in comparison to larger sand particles (In the range of 250-750 micron diameter). Localized corrosion attack in the presence of paraffin deposit is also negligible compared to silica sand deposit.

Key words: under-deposit, localized corrosion, inhibitor, sand, paraffin

INTRODUCTION

Under-deposit corrosion (UDC) has frequently been reported as a cause of failure in the oil and gas industry.¹ Under-deposit corrosion often results in severe localized corrosion attack; this is difficult to monitor, predict, and mitigate. Galvanic cells established between covered and uncovered regions of the metal surface, resulting in severe localized corrosion. Monitoring of localized corrosion is problematic because predicting the location of deposit formation is difficult and it happens along the pipeline in random locations. Mitigation is challenging because corrosion inhibitors do not efficiently protect the areas of the pipe covered by deposit. The inhibitors may even accelerate localized corrosion attack under deposits by the creation of more pronounced galvanic effects.² One of the best tools to mitigate under-deposit corrosion is pipeline pigging. It is important to mention that not every pipeline is piggable and even those lines that are piggable may suffer from extensive corrosion damage if the pigging frequency is not adequate.

Different types of deposits have been reported in the oil and gas industry. In 2005, de Reus, et al.³ reported that field deposits are most frequently silica sand associated with produced oil. Deposits can be divided into two main categories:

- a) Suspended solids, such as silica sand, in the production fluid
- b) Products of chemical, electrochemical, and physical reactions/processes

Calcium carbonate and barium sulfate are two examples of products that precipitate from aqueous species present in the pipeline. Iron sulfide and iron carbonate are products that form due to electrochemical corrosion reactions. Paraffin wax and asphaltene have the potential to deposit due to physical processes (i.e. change in temperature).

Previous research by Huang, et al.^{4,5} showed that a silica sand deposit does not cause any localized corrosion attack for API 5L X65 carbon steel when there is no corrosion inhibitor in the system. They also showed that silica sand deposit reduces the corrosion rate by limiting mass transfer of corrosive species to the metal surface, as well as limiting the mass transfer of corrosion products from the metal surface to the bulk solution. Therefore, water chemistry at the metal surface underneath the deposit can be significantly different from water chemistry in the bulk solution. Huang, et al. reported under deposit pH values 1-2 units higher than in bulk solution. They also reported less of an effect of bulk pH and temperature on the under-deposit corrosion rate because of limited diffusion and mass transfer through the deposit layers. This different water chemistry at the metal surface and higher pH under the silica sand deposit also promoted the formation of iron carbonate scales.

Huang, et al.⁵ also investigated the interaction of an imidazoline-type corrosion inhibitor with the silica sand deposit and showed that, partial coverage (less than 50% of surface covered) of sand particles larger than 150 μm (diameter) resulted in severe localized corrosion attack. The presence of sand has been reported as the cause of local removal of inhibitor from the metal surface, resulting in formation of galvanic cells between areas covered with inhibitor and crevice area under each sand particle without inhibitor. This accelerated the corrosion rate and caused severe localized attack. The driving force for this localized corrosion attack was reported to be in the region of 20-40 mV. The localized corrosion rate was also reported to be almost 5 - 10 times higher than the uninhibited uniform corrosion rate.

Nyborg et al.⁶ reported galvanic corrosion attack on a sand covered carbon steel specimen electrically coupled to a specimen without sand deposit when inhibitor was added to the system before the sand. Later, Pandarinathan, et al.⁷ showed that cationic surfactant corrosion inhibitors adsorb more on silica sand because of electrostatic attractions and interactions between alkyl groups; a secondary finding was that corrosion inhibitors containing sulfur showed less adsorption on silica sand. Tan, et al.² reported uniform corrosion under sand deposits when there was no inhibitor in the system, but the onset of localized corrosion occurred when an imidazoline-type inhibitor was added to the CO₂ system. They also reported that increasing the inhibitor concentration decreases the uniform corrosion rate, but accelerates the localized corrosion rate. Xue, et al.⁸ utilized localized electrochemical impedance spectroscopy and a scanning vibrating electrode to study the localized corrosion attack under silica sand deposit and reported pitting corrosion even without adding corrosion inhibitor to the system.

The main hypothesis of the current research is that small silica sand particles cause less under deposit localized corrosion attack as compared to larger silica sand particles because of a smaller cathodic to anodic surface area ratio (cathodic surface area is the area protected by inhibitor and anodic surface area is the area in the crevice space underneath the sand particle that inhibitor has been removed because of sand). Testing of this hypothesis permits further elaboration of under-deposit corrosion mechanisms previously proposed by Huang, et al.⁵

A second hypothesis was tested using a paraffin deposit. Due to their non-polar character, paraffin deposits are hypothesized to have less of an interaction with imidazoline-type inhibitors and, consequently, localized attack under such deposits is predicted to be negligible.

EXPERIMENTAL PROCEDURE

The electrochemical tests were performed in a 2 liter glass cell (Figure 1). API 5L X65 mild steel (about 8 cm²) was used as the working electrode. Deposit either covers the whole surface of the working electrode or more than 50%. A platinum wire was used as the counter electrode (about 10 cm²) and an Ag/AgCl (saturated KCl) electrode was used as the reference electrode. A glass pH probe was also immersed in the solution to monitor pH changes during the tests. The electrolyte in the glass cell was purged continuously with CO₂ during experiments to maintain the CO₂ partial pressure, to keep the solution saturated with CO₂, and to remove dissolved oxygen. A condenser was also used to prevent loss of fluid due to evaporation. A Gamry 600 potentiostat was used for electrochemical measurements. Oxygen concentration was measured and it was less than 20 ppb.

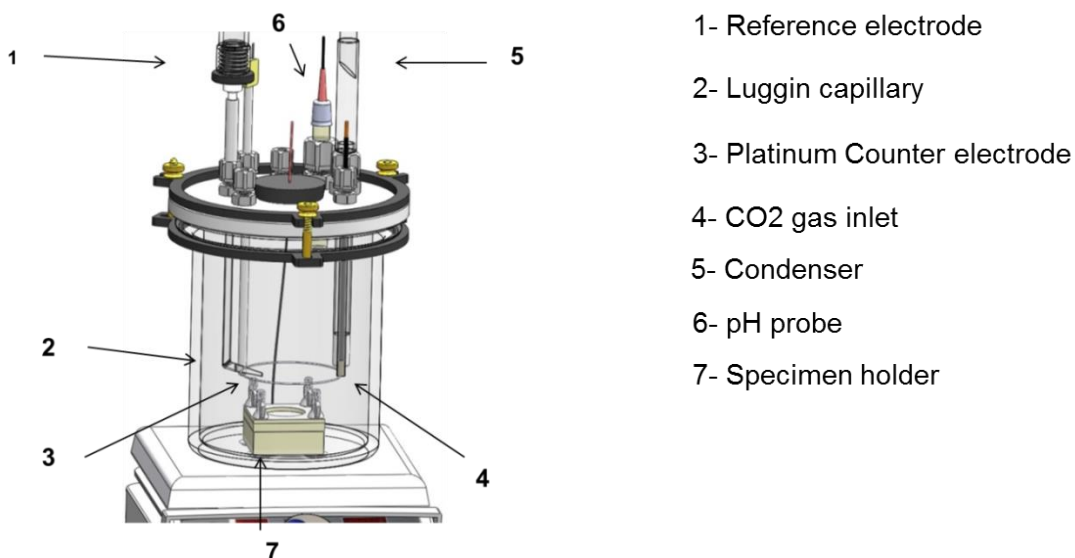


Figure 1: Schematic of glass cell setup for electrochemical measurements.⁹

Table 1 shows the material used for this research, experimental conditions, and the different techniques used for monitoring corrosion and analyzing specimens.

Table 1 Materials, test conditions, and analysis techniques

Parameter	Conditions
Material	API 5L X65
CO ₂ partial pressure	1 bar
Solution	1wt.% NaCl, pH 5.0 (adjusted using bicarbonate)
Type of Deposit	Silica sand (with three different sizes: <44, 250 and 750µm) and/or Eicosane paraffin
Deposit Depth/Characteristics	1.6 mm and partially covered (less than 50%)
Temperature	25°C
Corrosion Rate Measurement	Weight Loss (WL) Linear Polarization Resistance (LPR) ±5 mV vs. OCP (0.125 mV/s)
Surface Analyzing technique	Scanning Electron Microscopy (SEM) Surface Profilometry

The generic inhibitors used in these experiments were labelled K1 and K4; K1 has 24% TOFA/DETA imidazoline as the only active component and K4 is a blend of 20% TOFA/DETA imidazoline and 4% sodium thiosulfate. The concentration used in all cases was twice the critical micelle concentration (CMC), corresponding to 140 ppm for K1 and 430 ppm for K4. The CMC is the concentration of surfactants above which micelles form and all additional surfactants added to the system go to micelles.

Figure 2 shows the SEM image of the small particle silica sand, termed “silica flour”, used for this under-deposit corrosion study. The size of the particles was smaller than 44 μm .

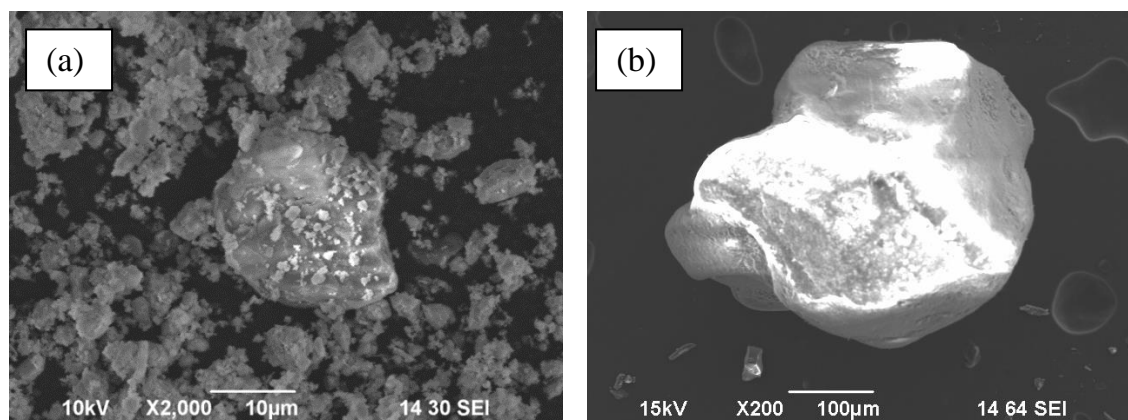


Figure 2: SEM image of silica flour (a) small sand particle (<44 μm) (b) large sand particle.

Experimental work was conducted in two different methods.

1. Short term exposure (*i.e.* 7 day) experiments were done in a two liter glass cell equipped for electrochemical measurements to monitor the solution resistance and uniform corrosion rate using linear polarization and impedance spectroscopy techniques. The iron ion concentration was also measured after experiments.
2. Long term exposure (*i.e.* 35 day) experiments were conducted in a one liter glass cell without any electrochemical measurements. However, the iron ion concentration was measured during experiments and pH was also adjusted to be constant at pH 5.0.

The steel specimens for the exposure tests were cylindrical with a surface area of 8 cm^2 . For the electrochemical measurements, the samples were mounted in a holder, where only the top surface of the steel sample was exposed to the environment, using an o-ring separating the rest of the cylinder from the corrosive environment. For the weight loss tests, the samples were coated on the sides and bottom with a Polytetrafluoroethylene (PTFE) paint before the polishing procedure.

In all cases, prior to each experiment, the specimens were sequentially polished with 200, 400 and 600 grit silica carbide (SiC) abrasive papers under a continuous rinse with isopropyl alcohol, air dried, then inserted into the sample holder. After adjusting the solution pH to 5.0 by gradual addition of deoxygenated sodium bicarbonate (NaHCO_3), the specimen holder was immersed into the prepared solution and the test was started at 25 $^\circ\text{C}$.

The sequence of addition of inhibitor and silica deposit is shown in Figure 3. The solution was purged with CO_2 for two hours then the carbon steel samples were added to the system. After two hours of pre-corrosion, the inhibitor was injected to the system. Then two hours after inhibitor injection, silica sand was deposited on the metal surface. In this experiment, specific production conditions were simulated in which the pipeline is protected by a corrosion inhibitor and then silica sand deposits at the bottom of pipe because of low flow velocity or system shut down.

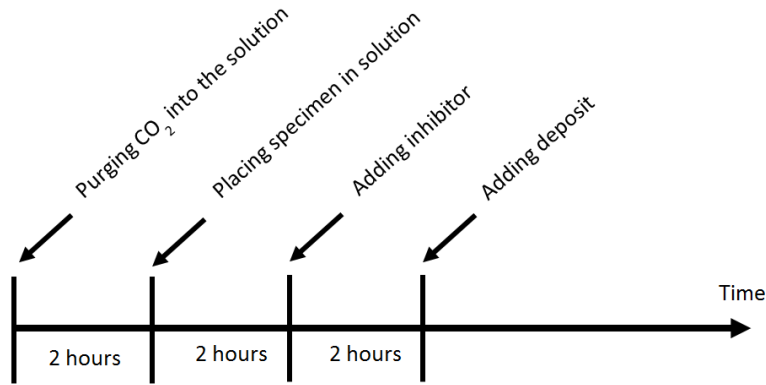


Figure 3 Sequence of experimental steps

Scanning electron microscopy (SEM) and surface profilometry were the two major techniques used for surface analysis to detect any localized corrosion attack.

RESULTS

Effect of Small Silica Sand on Localized Under Deposit CO₂-Corrosion

SEM images of localized under-deposit corrosion in the presence of small particle silica sand and imidazoline-type inhibitor are shown in Figure 4. The experiment duration was one week at 25°C and a pH of 5.0. Many small pits were observed on the metal surface, the diameters of which are smaller than 5µm. Surface profilometry for studying the depth of these features was not feasible because the depth of the features were in the error range of the device. Therefore, cross-section analysis of the specimens was performed using the SEM to measure the pit depth and to calculate the pitting rate (Figure 5).

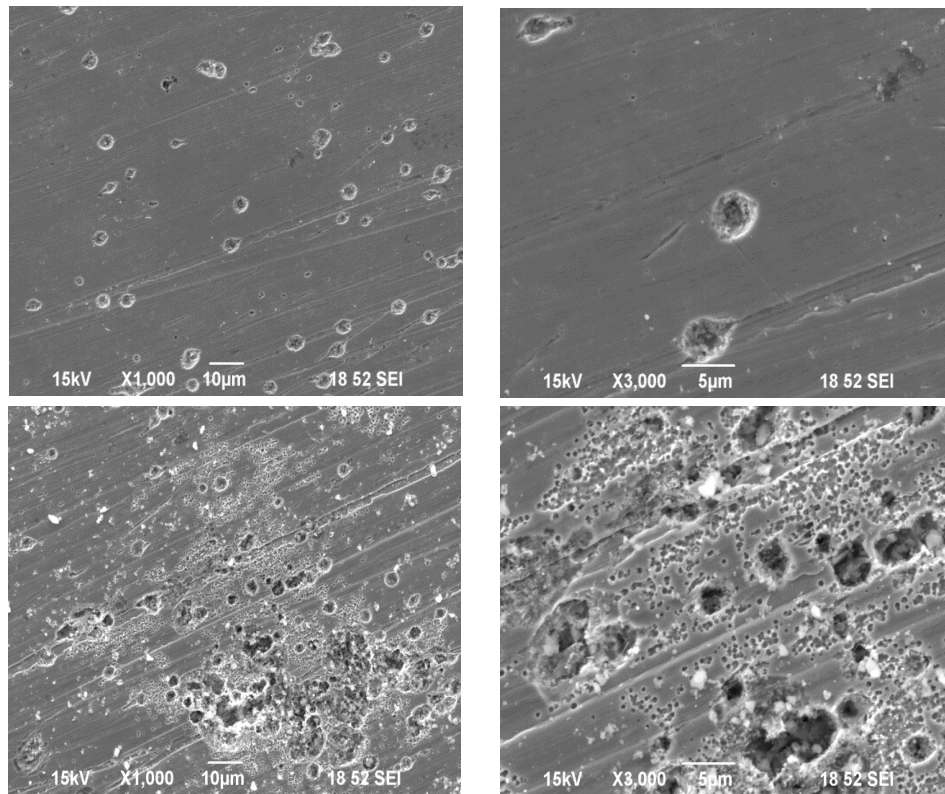


Figure 4: SEM images for top view of steel surface corroded under small sand particles in the presence of inhibitor K1 (1 week exposure)

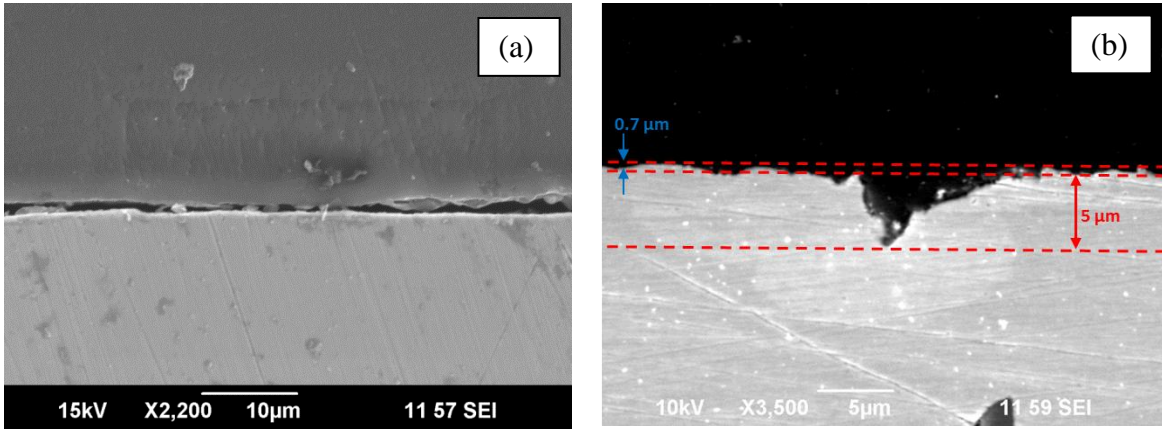


Figure 5: SEM image for cross section of X65 carbon steel (a) before corrosion experiment and (b) after localized corrosion attack under small sand particles in the presence of inhibitor K1 (1 week exposure)

Measurements of locally corroded areas revealed a rate of localized attack of 0.36 mm/yr. Uniform corrosion rate of the specimen was measured using electrochemical techniques and was determined to be 0.05 mm/yr, which corresponds to 0.7µm thickness loss for a week long corrosion experiment. Uniform corrosion rate under these conditions without inhibitor was 1.2 mm/yr. Therefore, the rate of localized corrosion attack in the presence of small sand particles (i.e. 0.36 mm/yr) is about a quarter of the uniform corrosion rate without inhibitor (i.e. 1.2 mm/yr). Huang et al.⁵ reported that the localized corrosion rate in the presence of larger sand particles is in the range of 2-3 mm/yr, which is higher than the uniform corrosion rate without inhibitor (Figure 6). It has to be mentioned that in previous work by Huang et al.⁵ sand particles were added first and then the inhibitor was added to the system. However, in this work inhibitor was added first to the system and then small sand particles were deposited on the surface. The sequence of adding sand and inhibitor also affects the localized corrosion rate underneath the sand to some extent.

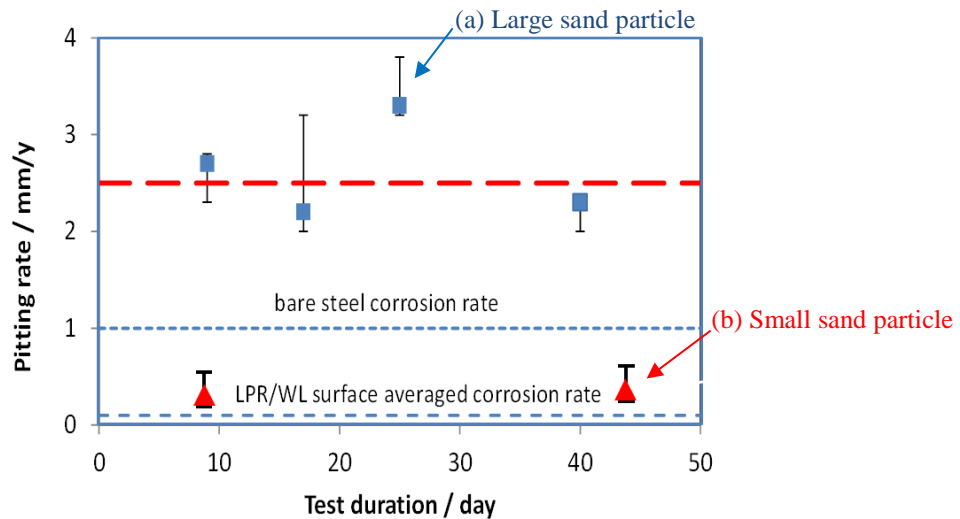


Figure 6: Uniform and localized corrosion rate with and without inhibitor and sand deposit: (a) Huang et al.⁵ large particle silica sand; (b) current work, small silica sand.

The deposit consisting of smaller sand particles showed a lower localized corrosion. The sequence of addition of sand and inhibitor to the system is an important factor on the severity of localized corrosion attack. It has been hypothesized that reduction to the inhibitor concentration can happen due to its adsorption on silica surfaces. In this case, the small particles would have a larger surface area than large particles when present with the same mass. This means more inhibitor can be adsorbed by the

smaller sand particle for the same weight concentration. However, the results suggest that bulk loss of inhibitor because of adsorption to the small sand particles was not the main mechanism of localized attack under sand deposits. This implies that the main mechanism of under deposit localized corrosion would be the formation of galvanic cells between cathodic and anodic sites on the surface, which are formed because of local loss of inhibitor near each sand particle (Figure 7).

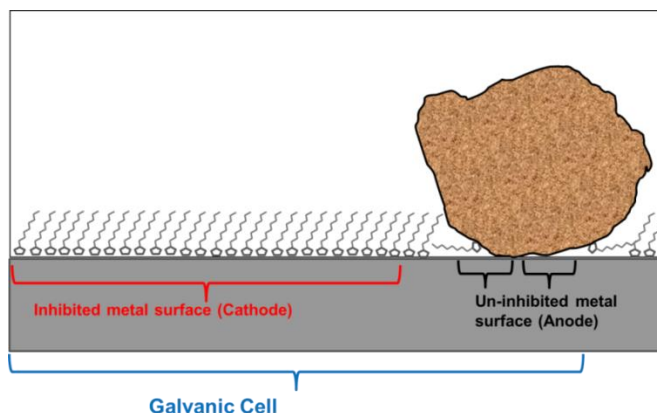


Figure 7: Schematic showing the formation of galvanic cell under sand deposit.

The difference in cathodic to anodic area ratio as related to sand particle size is depicted in Figure 8. A sand deposit with larger particles (Figure 8a) will have a higher porosity than a sand deposit with smaller particles (Figure 8b). When the inhibitor reaches the metal surface through the deposit, this difference in porosity supports the hypothesis that a group of larger sand particles would have fewer, larger cathodic areas (i.e. inhibited surface) in between sand particles while a group of smaller sand particles would have many, small, cathodic areas on the surface.

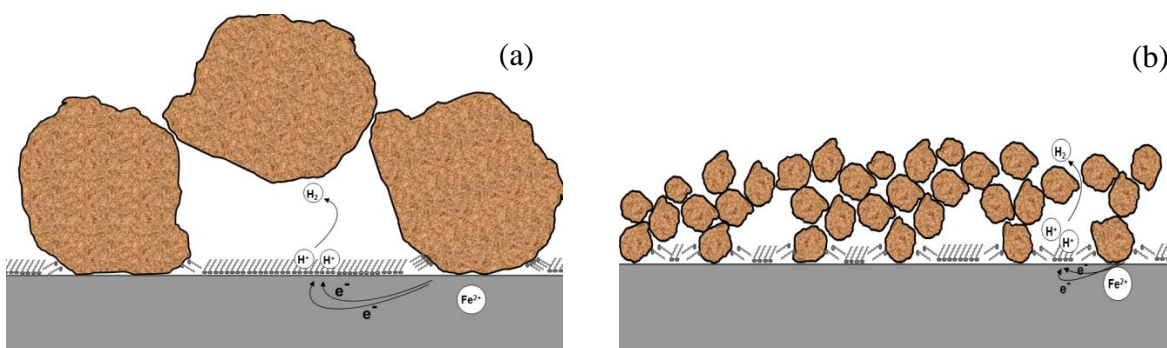


Figure 8: Schematic showing the formation of small galvanic cell underneath silica sand particles: (a) larger sand particles; (b) smaller sand particles.

Visual analysis by SEM agrees with this hypothesis is shown in Figure 9. Figure 9 shows a comparison of SEM images for localized corrosion under deposited silica for (a) large (750 μm) (Huang, et al.⁵) and (b) small (<44 μm) sand particles (note the difference in magnification of the SEM images). Both experiments were done at 25°C and pH 5.0 for about one month. The morphologies of the locally attacked areas are very similar. The appearance of the crevice edge and pit are very similar even though their diameter is more than two orders of magnitude different.

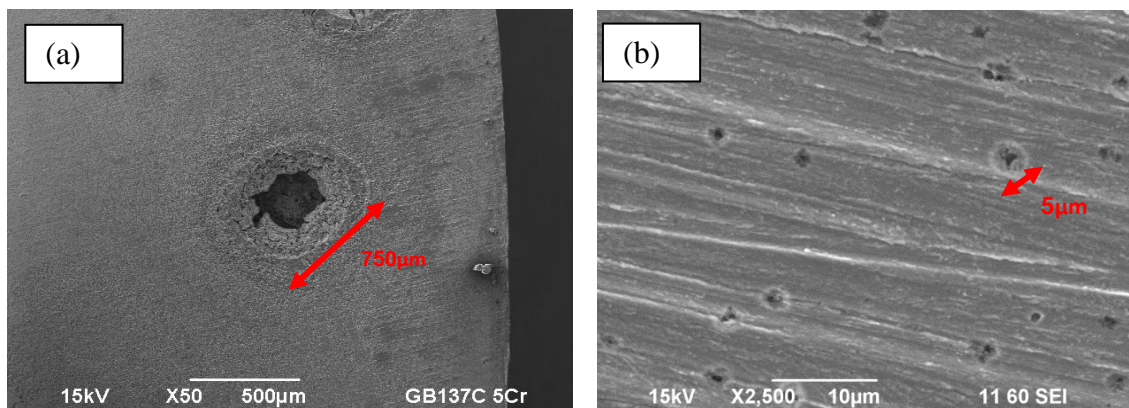


Figure 9: Localized corrosion under silica sand deposit (a) large silica sand, diameter of 750 μm (Huang, et al.⁵) (b) small silica sand (<44 μm), 1 month exposure.

Small space between the metal surface and silica particle is the starting point for the initiation of localized corrosion attack underneath the sand particles (Figure 10). Two main mechanisms are suggested for explaining the initiation of localized attack. Figure 10 (a) shows a schematic of such a small space between a silica sand particle and the metal surface into which inhibitor molecules fail to diffuse, resulting in failure to protect the metal surface. Smaller water molecules diffuse more readily into this small space. Therefore, there is an uninhibited metal surface immediately underneath the sand that develops into a crevice.

The second mechanism is preferential adsorption of inhibitor molecules by silica sand, as described in Figure 10b. This results in creation of metal surface without inhibitor protection, which becomes an anodic site, compared with the rest of the inhibited metal surface, which in turn becomes cathodic. Previous research by Tan, et al.² showed that adding more imidazoline-type inhibitor to the system not only fails to stop the localized attack underneath the sand deposit, but accelerates the localized attack. This is further evidence for the development of crevice space between silica sand particles and the metal surface into which extra inhibitor added to the system is unable to diffuse into and confer protection. Localized corrosion in this crevice space eventually permits the sand particle to progressively settle into, or gradually diffuse into the metal surface until the diameter of the localized attack feature is the same as the diameter of the silica sand particle. Eventually, there is no space left between the metal surface and silica sand. Previous research by Huang, et al.⁵ shows that the size of localized attack area is exactly equal to the diameter of silica sand particles (long-term experiments need to be run to see this effect). The fact that the geometry of localized attack features underneath the sand can be correlated to the geometry of the sand particles proves that the developed crevice space plays an important role in the initiation of localized attack underneath deposits.

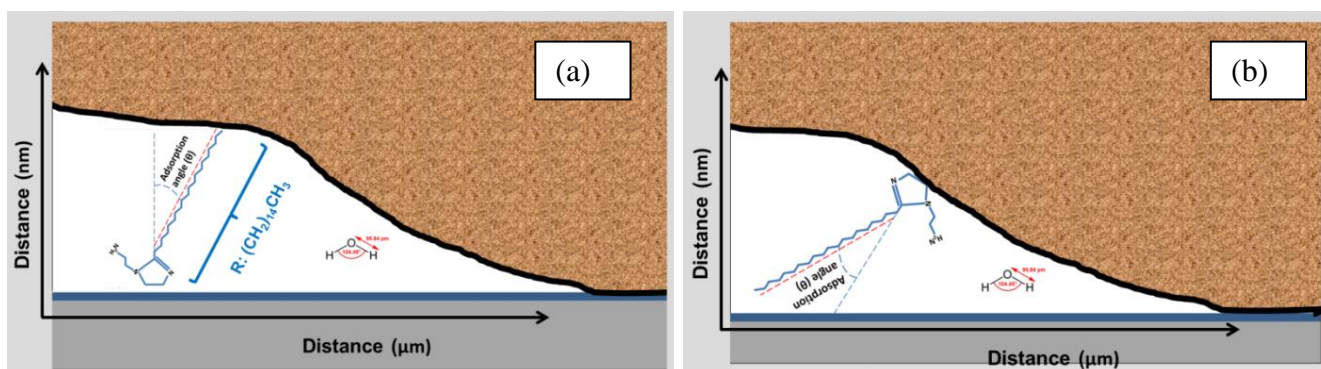


Figure 10: Schematics showing the local inhibitor loss at the interface between the silica sand particles and the metal surface a) inhibitor adsorption by metal surface b) inhibitor adsorption by silica sand.

Figure 11 shows the schematic of pit formation and propagation under a silica sand particle. SEM image of localized under-deposit corrosion attack published by Huang, et al.⁵ shows the formation of a pit exactly underneath, and at the center, of a deposited silica sand particle (Figure 12). The particle acts as a shield that limits access to the bulk environment, causing a difference in local surface conditions, and leading to the establishment of an electrochemical corrosion cell. This is similar to phenomena that occur in crevice corrosion, suggesting that mass transfer pathways at the crevice edge are an important factor in pit formation and propagation.

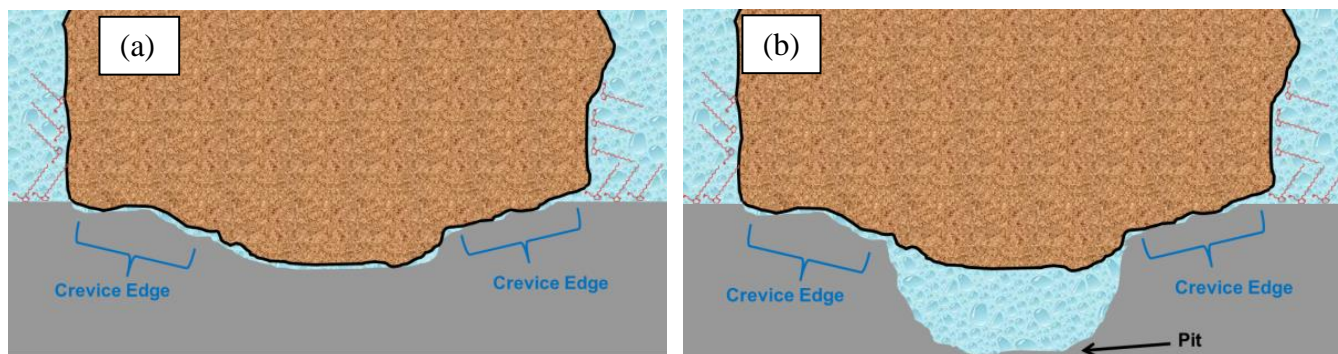


Figure 11: Schematic of pit formation under silica sand deposit (a) crevice edge underneath the sand particle limits inhibitor access to this location and causes crevice corrosion (b) crevice corrosion causes pit formation and propagation.

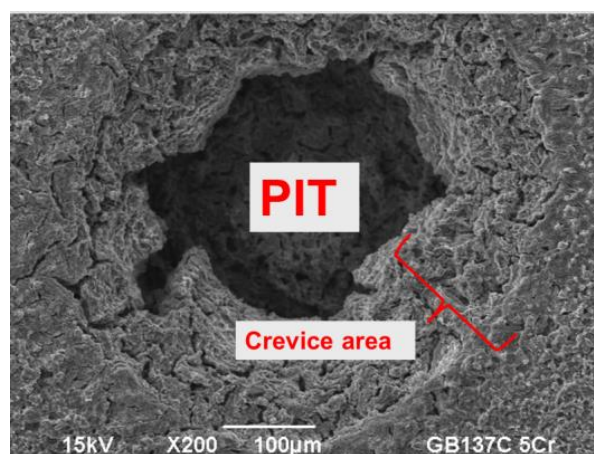


Figure 12: SEM image of localized corrosion attack area under silica sand deposit (Huang, et al.⁵)

Interaction of imidazoline-type inhibitor with paraffin underneath deposit

Figure 13 shows surface analysis using SEM for studying localized corrosion attack where interaction occurs between imidazoline-type inhibitor and paraffin underneath the deposit. Experiment duration was one week at 25°C and pH of 5.0. Slightly more corrosion was observed exactly at the interface between paraffin and the metal surface, but there was no sign of severe localized corrosion attack as was observed for silica sand.

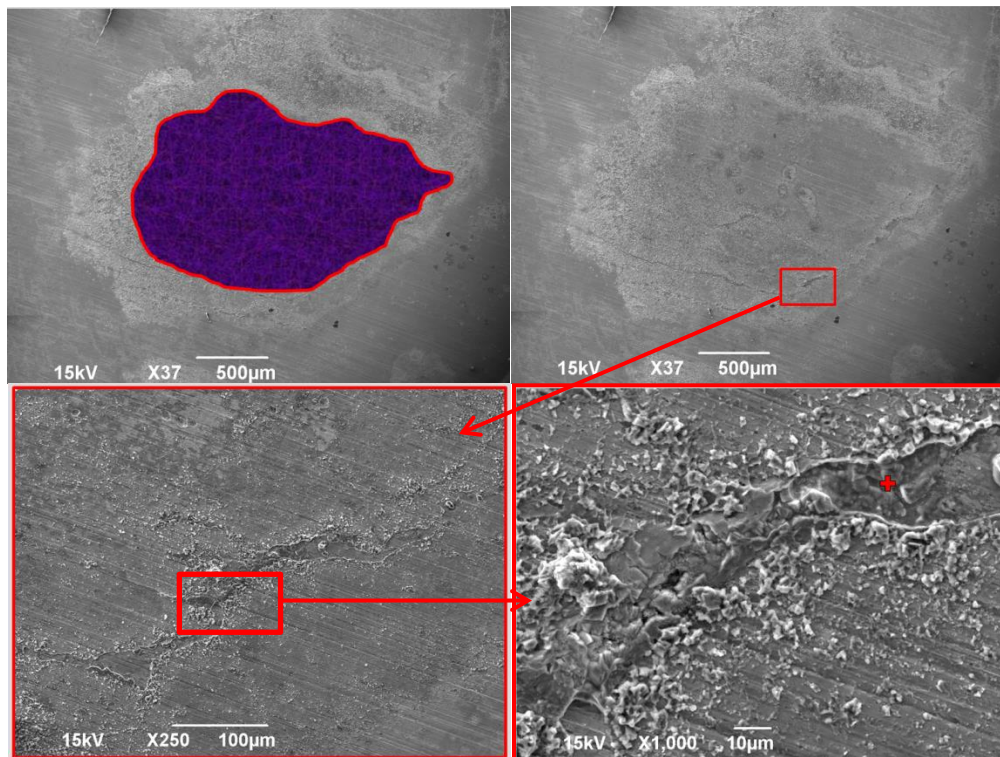


Figure 13: SEM images of a metal surface underneath paraffin at progressively higher magnifications (x37, x250, and x1000). 1 week at 25°C and pH of 5.0.

Figure 14 shows the comparison of LPR general corrosion rate data for two different samples partially covered with silica sand and paraffin. General corrosion rate in the presence of paraffin wax was lower than silica sand. The paraffin wax adheres to the metal surface, making it hydrophobic. This keeps water away from the surface and, consequently, reduces the corrosion rate by reducing the active surface area.

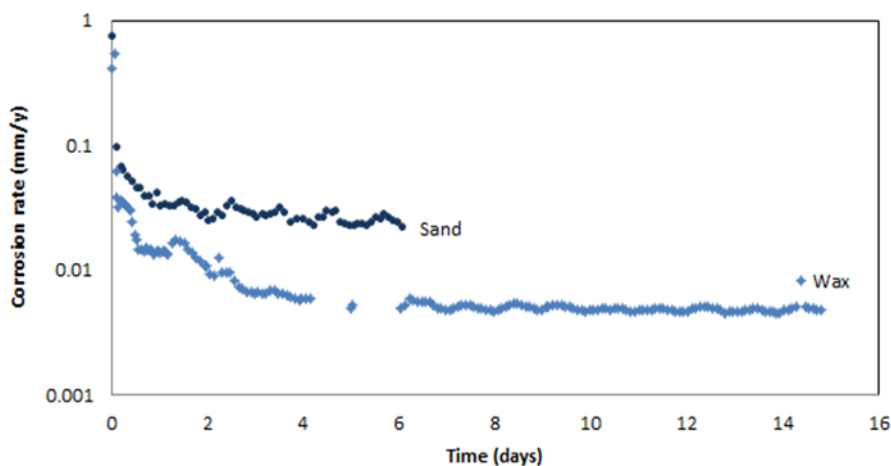


Figure 14: Comparison of LPR corrosion rate data for X65 carbon steel in the presence of silica sand and paraffin surface deposits at 25°C, 1 bar CO₂, and in the presence of 400 ppm K1 inhibitor.

The experiment was run for a longer time (35 days) to confirm the previous findings about no sign of severe localized attack underneath the paraffin deposit. Figure 15 shows SEM images of the surface at two different locations, right at the interface of the deposit and metal surface and also away from the deposit. It can be seen that away from the deposit there is no significant corrosion as polishing marks

can be clearly seen after 35 days of experiment, which means that imidazoline provides a good protection to the metal surface. However, right at the interface of the paraffin deposit and metal surface, slightly more corrosion was observed. It has to be mentioned that localized attack under the paraffin deposit was considerably lower than localized attack under the silica sand deposit. Experimental results show that preferential adsorption of corrosion inhibitor with paraffin is different than for silica sand. Also, because of the nature of the solids, the crevice space between paraffin and a metal surface is different from the crevice space between silica sand and a metal surface.

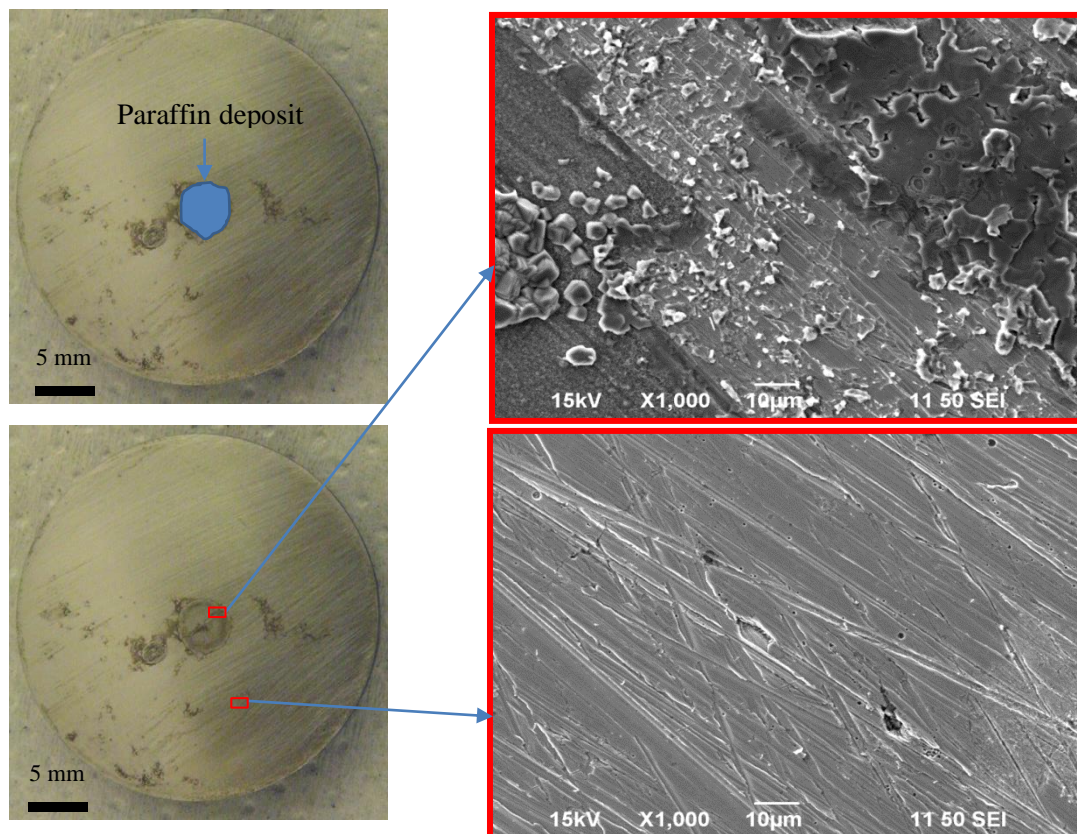


Figure 15: SEM image of the surface for 35 days long under paraffin deposit corrosion in the presence of K1 inhibitor at 25°C and pH 5.0.

CONCLUSIONS

1. Mechanisms of localized corrosion of carbon steel X65 in CO₂ environment under a silica sand can be summarized as follows:
 - a. The preferential adsorption of inhibitor by silica sand and the crevice space that occurs between a sand particle and the metal surface are two main factors leading to initiation and propagation of localized under-deposit corrosion in aqueous environments.
 - b. Pit propagation under a single silica sand particle allows the sand to sink into the metal surface until the diameter of the locally corroded area is equal to the sand particle diameter.
 - c. Each locally corroded site under a deposited silica sand particle consists of two main parts: crevice area and pit.
2. Localized corrosion in the presence of deposited small silica sand particles (<44 μm) was less severe as compared to larger silica sand particles.

3. Paraffin wax deposit reduced the uniform corrosion rate due to its adhesion to the surface; its presence does not result in any localized corrosion.
4. Paraffin, likely in association with the alkyl tail of the inhibitor molecule, makes the metal surface hydrophobic.
5. Experimental data showed that paraffin wax did not cause severe localized corrosion attack as seen with silica sand because it does not create a crevice space underneath the deposit.
6. Larger cathodic surface area slightly accelerated the localized corrosion attack depending on the conductivity of the solution and distance between cathodic and anodic sites.

ACKNOWLEDGEMENTS

The author would like to thank the following companies for their financial support: BP, Champion Technologies, Chevron, Clariant Oil Services, ConocoPhillips, DNV GL, ENI S.p.A., ExxonMobil, Hess, INPEX Corporation, MI-SWACO, Multi-Chem, NALCO Energy Services, Occidental Oil Company, Petrobras, PETRONAS, PTT, Saudi Aramco, Total, TransCanada Pipelines, Ltd., and WGIM.

REFERENCES

1. J. R. Vera, D. Daniels and M. H. Achour, "Under-deposit corrosion (UDC) in the oil and gas industry: A review of mechanism, testing and mitigation," in NACE International, 2012.
2. Y. Tan, Y. Fwu and K. Bhardwaj, "Electrochemical evaluation of under-deposit corrosion and its inhibition using the wire beam electrode method," *Corrosion Science*, pp. 1254-1261, 2011.
3. J. de Reus, E. Hendriksen, M. Wilms, Y. Al-Habsi, Y. Durine and M. Gough, "Test methodologies and field verification of corrosion inhibitors to address under-deposit corrosion in oil and gas production systems," in NACE Corrosion International, 2005.
4. J. Huang, B. Brown, X. Jiang, B. Kinsella and S. Nescic, "Internal CO₂ corrosion of mild steel pipelines under inert solid deposits," in NACE Corrosion International, 2010.
5. J. Huang, B. Brown and S. Nescic, "Localized corrosion of mild steel under silica deposits in inhibited aqueous CO₂ solutions," in NACE Corrosion International, 2013.
6. R. Nyborg and M. Foss, "Experience with an under-deposit corrosion test method with galvanic current measurements," in NACE Corrosion International, 2011.
7. V. Pandarinathan, K. Lepkova, S. Bailey and Gubner, "Evaluation of corrosion inhibition of sand-deposited carbon steel in CO₂-saturated brine," *Corrosion Science*, pp. 108-117, 2013.
8. H. Xue, F. Cheng, N. Tajallipour and P. Teevens, "Internal pitting corrosion of X80 pipeline steel under deposited sand bed in CO₂-saturated solutions," in NACE Corrosion International, 2011.
9. J. Huang, Mechanistic study of under-deposit corrosion of mild steel in aqueous carbon dioxide, PhD Dissertation, Ohio University, 2013.
10. J. Huang, B. Brown, Y. Choi and S. Nescic, "Prediction of uniform CO₂ corrosion of mild steel under inert solid deposits," in NACE Corrosion International, 2011.